5144 J. Med. Chem. 2009, 52, 5144–5151
DOI: 10.1021/jm900277z

Journal of Medicinal Chemistry Article

Identification of Enoxacin as an Inhibitor of Osteoclast Formation and Bone Resorption by Structure-Based Virtual Screening

David A. Ostrov,[†] Andrew T. Magis,[†] Thomas J. Wronski,[‡] Edward K. L. Chan,[§] Edgardo J. Toro,[∥] Richard E. Donatelli,[∥] Kristen Sajek,[∥] Ireni N. Haroun,[∥] Michael I. Nagib,[∥] Ana Piedrahita,[∥] Ashley Harris,[∥] and L. Shannon Holliday*[,∥,⊥]

[†]*Department of Pathology, Immunology and Laboratory Medicine, University of Florida College of Medicine, Gainesville, Florida 32610,* [‡]*Department of Physiological Sciences, University of Florida, Gainesville, Florida 32610,* [§]*Department of Oral Biology, University of Florida College of Dentistry, Gainesville, Florida 32610,* [∥]*Department of Orthodontics, University of Florida College of Dentistry, 1600 SW Archer Road, CB 100444, D7-18, Gainesville, Florida 32610, and* [⊥]*Department of Anatomy & Cell Biology, University of Florida College of Medicine, Gainesville, Florida 32610*

Received March 4, 2009

An interaction between the B2 subunit of vacuolar H^+-ATPase (V-ATPase) and microfilaments is required for osteoclast bone resorption. An atomic homology model of the actin binding site on B2 was generated and molecular docking simulations were performed. Enoxacin, a fluoroquinolone antibiotic, was identified and in vitro testing demonstrated that enoxacin blocked binding between purified B2 and microfilaments. Enoxacin dose dependently reduced the number of osteoclasts differentiating in mouse marrow cultures stimulated with 1,25-dihydroxyvitamin D_3, as well as markers of osteoclast activity, and the number of resorption lacunae formed on bone slices. Enoxacin inhibited osteoclast formation at concentrations where osteoblast formation was not altered. In summary, enoxacin is a novel small molecule inhibitor of osteoclast bone resorption that acts by an unique mechanism and is therefore an attractive lead molecule for the development of a new class of antiosteoclastic agents.

Introduction

Bone quality is maintained by a balance between bone resorption by osteoclasts and bone formation by osteoblasts.[1] Excess bone resorption can occur systemically, where it leads to osteoporosis,[2] or locally, where it is associated with bone tumors,[3,4] infections,[5−7] and inflammatory responses.[2,5,7] Although various agents are available for the treatment of excess osteoclast activity, none are ideal for the treatment of the associated pathologies.

Osteoclasts are specialized cells of the hematopoietic lineage.[8] Unusual features of osteoclasts include overexpression of vacuolar H^+-ATPases (V-ATPases[a]) and the transport of V-ATPases to the plasma membrane.[9,10] While V-ATPases are expressed in all nucleated eukaryotic cells, where they are responsible for acidification of compartments of the endocytic pathway, V-ATPases are normally present at low levels and are forbidden to entry into the plasma membrane.[11] The mechanisms underlying the overexpression of V-ATPases and their transport to the plasma membrane represent potential targets for therapeutic intervention that might be selective for osteoclast bone resorption.

We previously identified a binding interaction between V-ATPase subunit B2 and microfilaments in osteoclasts that correlates with the state of osteoclast activation. This interaction is mediated by a specific region of the B-subunit.[12−14] This region is called the "profilin-like domain" (amino acids 29−73 in B2 of mammals) based on sequence and structural similarity with the actin binding protein, profilin.[15] Minimal alterations to the profilin-like domain of the B-subunit disrupt actin binding activity without interfering with the capacity of the altered B-subunit to contribute to the enzymatic activity of the multisubunit V-ATPase.[14,16] B-Subunits so altered were not transported to the plasma membrane of osteoclasts.[17] Together, these data led us to hypothesize that small molecules that bind to the actin binding site on subunit B2 and interfere with its binding interaction with microfilaments might represent a new class of antiosteoclastic therapeutic agents. To identify such agents and test this hypothesis, we performed a virtual screen where each one of approximately 140000 small molecules (mw $<$ 500) were positioned in the selected structural pockets of the actin binding site of B2 and scored based on predicted polar and nonpolar interactions. This screen identified the fluoroquinolone antibiotic enoxacin as a candidate small molecule that may interact with the actin binding site of B2. In vitro assays demonstrate that enoxacin blocks the interaction between B2 and microfilaments and inhibits osteoclast formation and activity in a well characterized model system.

Results and Discussion

To identify small molecules that block the interaction between V-ATPase and F-actin in osteoclasts, we screened for drug-like small molecules that bind the actin binding site on the B subunit by molecular docking. We focused on small molecules that follow the Lipinski rules of drug-likeness

*To whom correspondence should be addressed. Phone: (352) 273-5689. Fax: (352) 846-0459. E-mail: sholliday@dental.ufl.edu.

[a] Abbreviations: V-ATPase, vacuolar H^+-ATPase; MBP, maltose-binding protein; 1,25D3, 1,25-dihydroxyvitamin D3; TRAP+, tartrate-resistant acid phosphatase positive.

 Published on Web 07/24/2009

(chemical parameters for orally bioavailable drugs) in a large chemical library (approximately 140000 compounds) at the National Cancer Center Developmental Therapeutics Program. In silico screens of large chemical libraries are taking on an increasingly prominent role in the rational design of pharmacological agents. Although such screens can reduce the number of candidate molecules to be tested, they are not yet able to predict with certainty whether molecules will interact with target domains on proteins.

The site selected for molecular docking was based on crystal structures of the profilin 1-actin complex.[18] Because part of the actin binding region of subunit B2 shares sequence homology with the actin binding site of profilin 1, and because the actin binding site of B2 and profilin 1 compete for binding actin,[14] we reasoned that the actin binding surfaces were likely similar. This was further confirmed by our analysis of single amino acid substitutions in the actin binding domain of the B2-subunit.[14] This information allowed us to identify the specific binding pockets of subunit B2 that were most likely required for the interaction with actin.

Each of approximately 140000 small molecules was docked into the putative actin binding site of the modeled human B2 subunit (Figure 1). Among the top 100 ranked small molecules was enoxacin which ranked seventh. We initially screened 19 of the top ranked small molecules for their ability to inhibit interaction between rabbit muscle actin and *Vma2p*-MBP.[16] *Vma2p*, the B subunit of *Saccaromyces cerevisiae,* has identical sequence to human B2 in the actin binding site and is readily purified after expression in *Escherichia coli*. Enoxacin was the most potent inhibitor of this interaction tested during this screen (Figure 2A). To demonstrate that this small molecule also inhibited the interaction between human B2 subunit and microfilaments, we performed the same assay using a fusion protein composed of maltose binding protein linked to amino acids 1−112 of human B2. We found that enoxacin dose dependently inhibited the interaction between MBP-B2 and F-actin with an IC_{50} of 10 μM (Figure 2B).

To determine the effects of enoxacin on osteoclasts, we made use of 1,25-dihydroxyvitamin D_3 ($1,25D_3$)-stimulated mouse marrow cultures, a widely utilized and well-characterized model of osteoclast differentiation and bone resorption. Mouse B2 is identical in sequence to human B2 in the actin binding region. After 7 days, the cells were fixed and stained for TRAP activity. Enoxacin dose dependently reduced the number TRAP+ cells (Figure 3A). Quantitation of the number and size of TRAP+ cells was performed. The number of giant cells, the best marker for osteoclast formation in these cultures was reduced by enoxacin with an IC_{50} in the low micromolar range (Figure 3B).

We then examined whether enoxacin would block actin ring and ruffled membrane formation by mature osteoclasts on bone slices. These are two robust and easily assayed markers of resorptive osteoclasts. Mouse marrow was cultured for 5 days in the presence of $1,25D_3$, to induce osteoclast formation, then loaded atop bone slices and treated with 1, 10, and 100 μM enoxacin. Enoxacin at 1 μM had no detectable effect on the numbers of actin rings and ruffled membranes exhibited by osteoclasts, but 10 and 100 μM reduced the number of both structures (Figure 4).

To test whether enoxacin inhibited bone resorption, mouse marrow cultures were treated with vehicle, 10, 25, or 100 μM enoxacin for 5 days, then loaded atop bone slices for an additional 5 days with continued enoxacin treatment

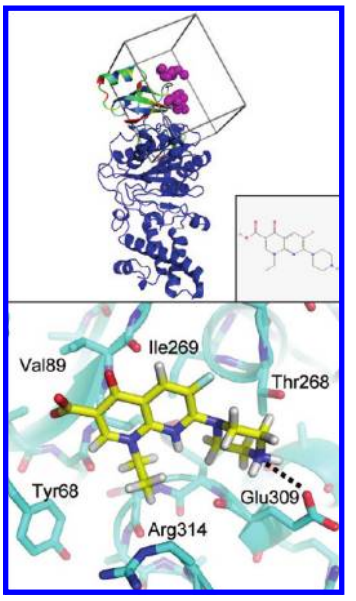

Figure 1. Identification of enoxacin by molecular docking. A homology model of human V-ATPase subunit B is shown in the top panel colored based on sequence similarity to profilin-1 (graded blue, cyan, green, yellow, orange, red to represent low sequence similarity (blue) to high (red) based on a BLOSUM62 matrix. Magenta spheres depict the site selected for molecular docking. The box represents boundaries of the scoring grid used for molecular docking. The chemical structure of enoxacin is shown in the inset of the top panel. The bottom panel shows enoxacin in the orientation posed by molecular docking using DOCK6.1 (UCSF), yellow for carbon, blue for nitrogen, red for oxygen, light blue for fluorine, white for hydrogen. The molecular surface of the V-ATPase B2 is colored cyan for carbon, blue for nitrogen, red for oxygen. Enoxacin may interact with a structural pocket in V-ATPase comprised of side chains from Tyr68, Val89, Thr268, Ile269, Glu308, and Arg314. In addition to van der Waals contacts between these residues and enoxacin, a H bond interaction is predicted between the Oε1 atom of Arg314 and N4 of enoxacin.

(Figure 5). No resorption was detected in cultures treated with 100 μM enoxacin. Enoxacin (25 μM) reduced both resorptive area and the number of pits formed significantly. At 10 μM enoxacin, there was a small, but significant, reduction in the number of pits formed (Figure 5).

We then examined whether the number of osteoblasts generated by the cultures was affected by enoxacin. Osteoblasts were detected by alkaline phosphatase activity. Enoxacin at 1 and 10 μM had no detectable effect on osteoblast number or morphology, while 100 μM strongly reduced the number of osteoblasts (Figure 6A). To confirm this result, we examined the effects of enoxacin on MC3T3-E1 osteoblasts cells. We detected no change in the growth of MC3T3-E1 cells or their expression of alkaline phosphatase activity at concentrations of enoxacin to 50 μM. At 100 μM, the cell displayed reduced growth and some alteration in their morphology (Figure 7B). Likewise, mineralization was unaffected by enoxacin (Figure 6C).

The fact that inhibition of the interaction between the B subunit and F-actin in biochemical assays and inhibition of osteoclast formation and bone resorption occurred in a similar concentration range is consistent with the results emanating from the same activity. However, during the course of the study, it was reported that enoxacin and some related fluoroquinolones stimulate RNA interference and enhance

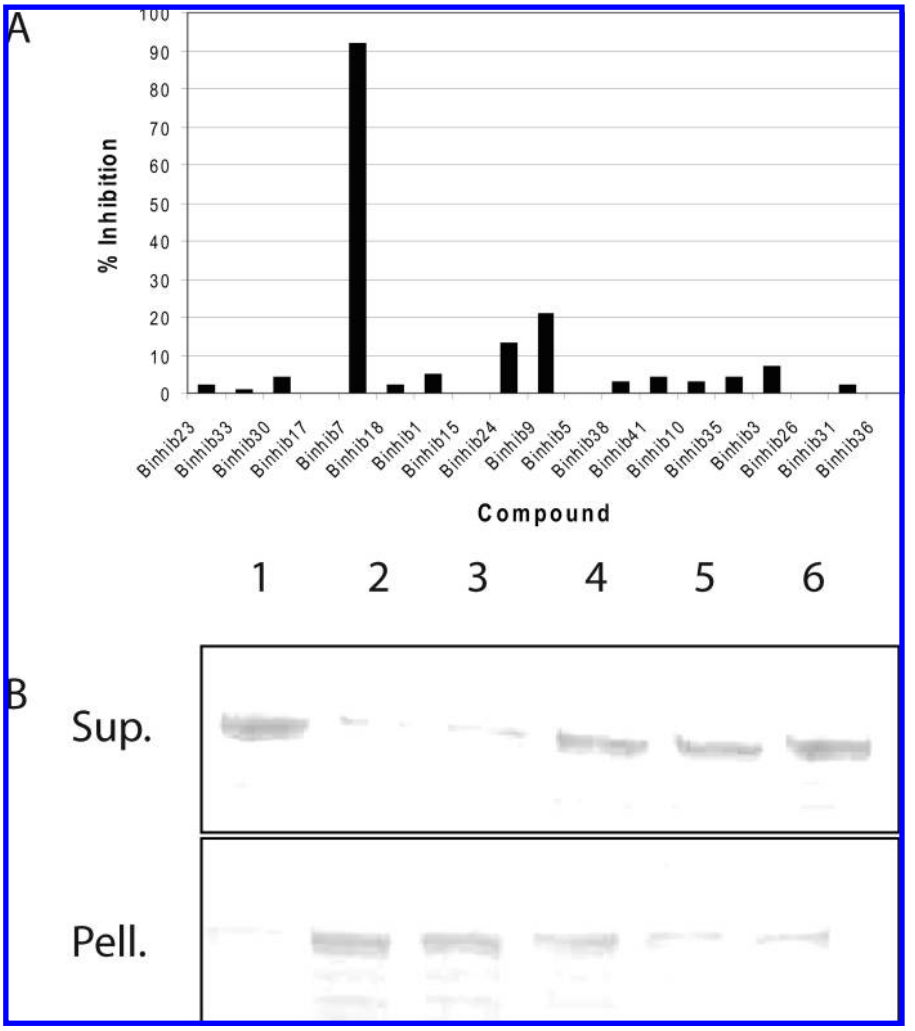

Figure 2. (A) Percent inhibition generated from pelleting assays for 19 small molecules tested at 100 μM concentration is shown. (B) Human B2 subunit (amino acids 1−112) at 1 μM concentration was mixed with 2 μM of microfilaments and pelleted in the presence of the following concentrations of enoxacin: (1) no actin control, (2) vehicle control, (3) 1 μM enoxacin, (4) 10 μM enoxacin, (5) 25 μM enoxacin, (6) 100 μM enoxacin. The amount of B2-MBP in supernatants and pellets is shown.

microRNA activity, also in a similar dose range.[19] MicroRNAs are a recently identified class of endogenously produced small RNAs that are thought to "fine tune" gene expression by binding to mRNAs and preventing their translation by sequestering them or triggering their degradation.[20] Evidence was provided suggesting that enoxacin might interact with human immunodeficiency virus-1 transactivating response RNA-binding protein, a protein involved in loading the RNA-induced silencing complex.[19]

It seems unlikely (but not impossible) that stimulation of microRNA activity could be the result of disruption of the interaction between V-ATPase and F-actin. Stimulation of microRNA activity, regardless of the mechanism, could affect osteoclast differentiation. To explore this, we assayed several fluoroquinolones for their ability to affect the interaction between V-ATPase and F-actin in vitro and to inhibit osteoclast formation. These included norfloxacin, which was reported to stimulate microRNA activity and others (pefloxacin and levofloxacin) that did not.[19,21] We found that only pefloxacin had a detectable effect on the interaction between B-subunit and F-actin (Figure 7A). Pefloxacin inhibited osteoclast formation, with an IC_{50} of about 50 μM compared with 10 μM for enoxacin (Figure 7B). The fact that norfloxacin, which also stimulates microRNA activity to similar levels as enoxacin,[19,21] but does not block V-ATPase−F-actin interactions, had no effect on osteoclast differentiation suggests that the microRNA stimulation activity is not important in inhibiting osteoclast differentiation at the concentrations tested. This interpretation was further supported by the ability of pefloxacin, which does not stimulate microRNA activity,[21] to block the V-ATPase−F-actin interactions and inhibit osteoclast formation. Taken together, these data are consistent with direct interference with the interaction between subunit B2 of V-ATPase and microfilaments being responsible for the inhibition in osteoclast formation.

The use of systemic enoxacin as an antibiotic has been linked to a number of adverse side effects.[22−24] These include phototoxicity, neurological problems, severe tendinitis, adverse immune activity, and renal failure due to distal renal tubular sensitivity. The capacity of enoxacin to block interactions between V-ATPase and microfilaments could represent an underlying mechanism for these adverse consequences. V-ATPases are key housekeeping enzymes, yet in certain specialized cell types, subpopulations of V-ATPases are vital for cell type specific functions. For example, in both

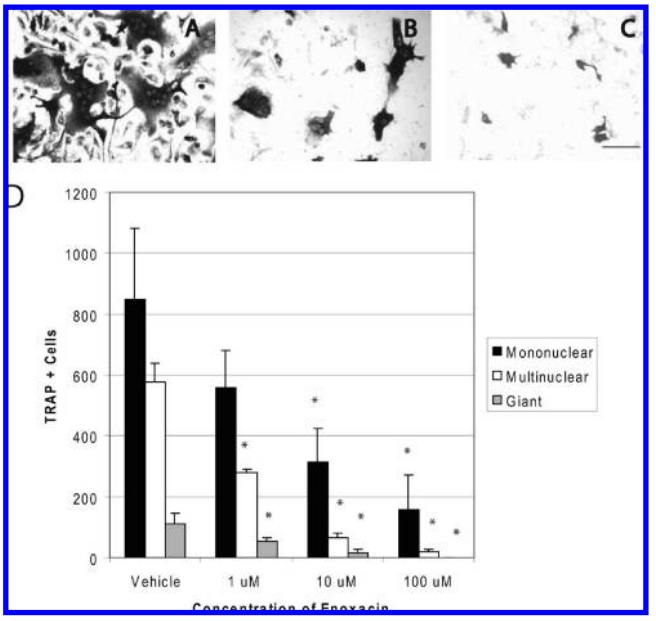

Figure 3. Enoxacin inhibits the number of TRAP+ cells differentiating from mouse marrow cultures. (A−C). Comparison of typical fields from mouse marrow cultures treated with calcitriol to stimulate osteoclast formation and (A) vehicle, (B) 10 μM, and (C) 100 μM enoxacin for 7 days. (D) Numbers of TRAP+ cells per well categorized by number of nuclei differentiating in response to calcitriol in the presence of varying concentrations of enoxacin. Asterisks indicate $P < 0.05$ compared with control value by Student's t test. Scale Bar = 30 μm.

osteoclasts and epithelial cells of the renal distal tubule, V-ATPases are expressed at high levels and inserted into the plasma membrane in order to pump protons from the cytosol to the extracellular environment.[25] In neurons, V-ATPases are associated with loading neurotransmitters into vesicles and with the fusion of those vesicles with the presynaptic plasma membrane.[26] Further studies will be required to examine the potential utility, as well as adverse effects, of enoxacin and related molecules.

In summary, we report the identification of enoxacin as an inhibitor of osteoclast formation and function by making use of a rational structure-based approach, utilizing molecular docking of a large chemical library in combination with biochemical and tissue culture assays. Our data suggest that enoxacin inhibits osteoclasts by a novel mechanism, blocking a binding interaction between the V-ATPase and microfilaments. V-ATPase activity is vital to osteoclast function, but because V-ATPase is expressed at low levels by all eukaryotic cells and performs housekeeping functions, efforts to use inhibitors of the proton pumping activity of V-ATPase to block bone resorption have not yet been successful. However, the interaction between V-ATPase and microfilaments has not been observed in most cell types studies but appears crucial for osteoclast function. We therefore reasoned that blocking the interaction might selectively inhibit osteoclastic bone resorption. Our data to date support this concept and encourage us to advance enoxacin as a lead molecule in the development of more potent and specific inhibitors of the interaction between V-ATPase B2-subunit and microfilaments as a new class of antiresorptive agents.

We aim to identify safe and effective small molecules that represent a new class of antiosteoclastic agents that block bone resorption by two distinct strategies. First, we will analyze a series of 20 structural variants of enoxacin in structure−activity relationship studies. The most active compounds in this series will be elaborated (derivatized) and compared with the activity of parent compounds in blocking the B-subunit−F-actin binding interaction and in blocking osteoclast formation in vitro.

A separate strategy involves docking all FDA approved small molecules in the V-ATPase structural pocket comprised of Tyr68, Val89, Thr268, Ile269, Glu308, and Arg314. Additional FDA approved drugs (approved for other purposes) are expected to be identified. Because these compounds are approved for use, this strategy may rapidly result in evaluation in clinical trials.

Experimental Section

Molecular Docking. An atomic homology model of the V-ATPase subunit B was generated by Swiss-Model (protein structure homology modeling using SWISS-MODEL workspace[27] based on the human sequence gi|13938355. Each of approximately 140000 small molecules in the "plated set" at the National Cancer Center Developmental Therapeutics Program repository of small molecules were positioned in the selected structural pockets of the B2 structural model in approximately 2000 different orientations and scored based on predicted polar and nonpolar interactions. Our strategy is described in greater detail below. Intermolecular AMBER energy scoring (vdw + columbic), contact scoring, and bump filtering were implemented in DOCKv6.1.0.[28] All molecular docking jobs were performed by parallel processing using 16 CPU on the High Performance Computing Center at the University of Florida running DOCK (UCSF) in Linux. Analysis of docked compounds was performed with HBPLUS and LIGPLOT.

The B-subunit of V-ATPase interacts with F-actin by a binding site that includes a stretch of 11 amino acids that is similar to the actin-binding site of profilin I, and this binds actin independently as a peptide.[14] In addition, when phenylalanine at position 65 in B2 was mutated to alanine, the binding affinity decreased 6-fold.[14] This was the target we chose to dock against in an attempt to inhibit the binding of V-ATPase to F-actin. To accomplish this, we created a homology model of V-ATPase with the Imperial College London Phyre server, using the known structure of profilin bound to beta-actin (PDB code 2BTF). We then ran the PDBSIM program to color the homology model by conservation, and predictably the phenylalanine 65 in question was colored as conserved. We targeted a pocket adjacent to this residue with our database of small molecules. The original sequences of V-ATPase and profilin were analyzed by the EMBL-EBI program ClustalW, which reproduced the alignment used for the docking job. The sequences are 17% identical, but including conserved and semiconserved substitutions, the sequences are 53% similar. This alignment is a 92-residue subset of both proteins which includes the putative F-actin binding sites. Using the atomic coordinates of both the V-ATPase homology model and the profilin crystal structure, we used the University of Illinois molecular viewer VMD to align the structures by backbone and measure the root-mean-square distance (rmsd). Total rmsd was 13.1 Å.

The scored orientations of each ligand were determined by DOCK. Each orientation was judged valid once it has passed the bump filter, indicating no major steric overlaps had been identified. An upper limit was set on the number of orientations used due to constraints in computer resources, particularly because a database of several hundred thousand molecules was being searched. We used 2000 orientations for

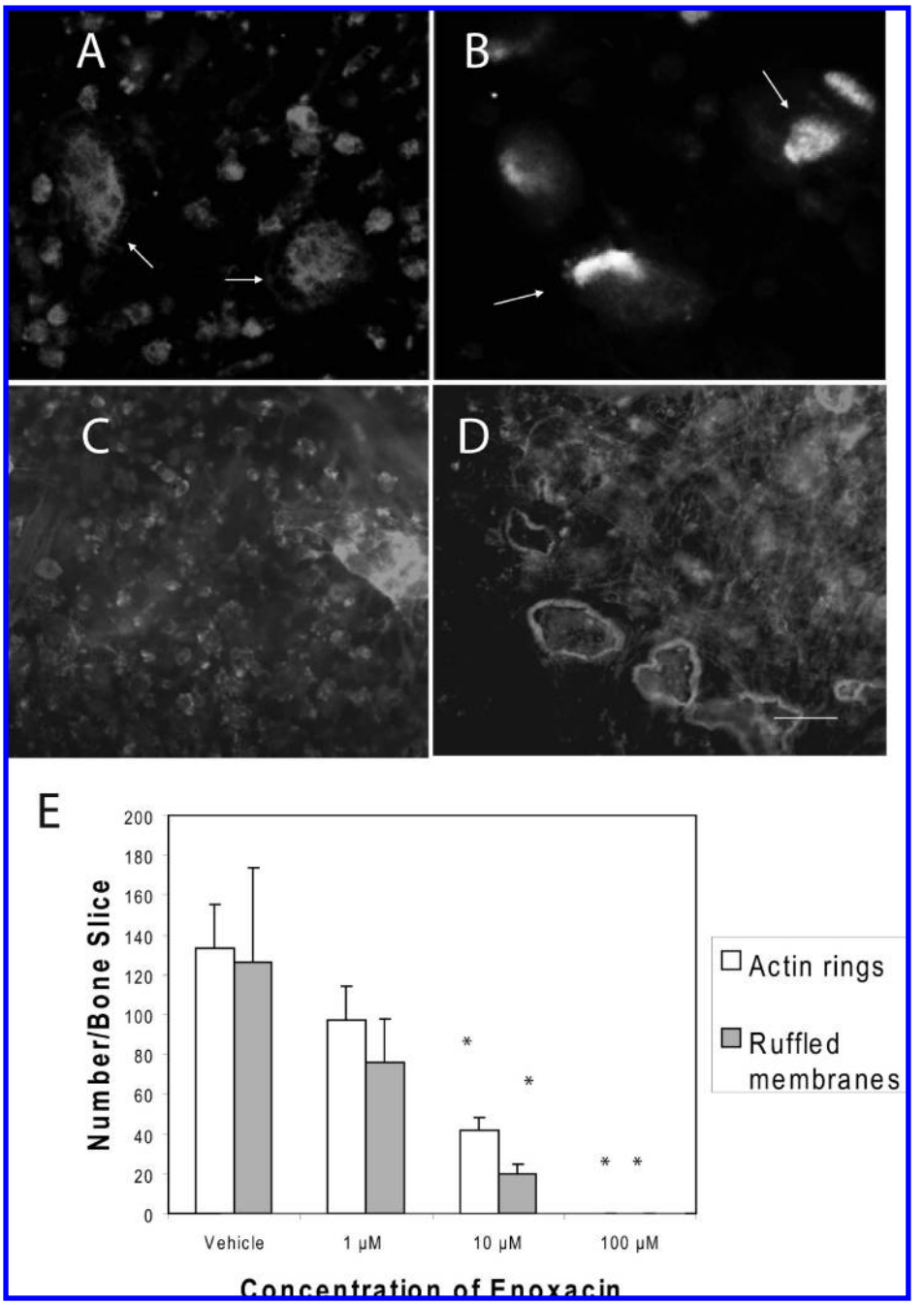

Figure 4. Treatment of mature osteoclasts with enoxacin reduced actin ring and ruffled membrane formation. Mouse marrow cultures on tissue culture plates were stimulated with calcitriol to for 6 days to produce osteoclasts. The cells were then scraped free and loaded atop bone slices and treated with vehicle or enoxacin as indicated. After 3 days, the cells were fixed and stained with anti-E subunit antisera to detect ruffled membranes (A,B) and with phalloidin to detect actin rings (C,D). B and D are typical fields from vehicle control cultures. A and C are fields from cultures treated with 100 μM enoxacin. Tabulation fo actin rings and ruffled membranes shows that both were reduced in a dose dependent manner by enoxacin. Asterisks indicate $P < 0.05$ compared with control value by Student's *t* test.

this docking job. Each initial orientation then went through two rounds of energy minimization using the DOCK simplex minimization routines. These calculations involved choosing up to 100 random permutations of the initial docked orientation in an attempt to improve the energy score, which terminates when the maximum number of permutations is reached or the energy score converges. For the 2000 orientations used, up to 200000 conformations per molecule were searched.

An energy based scoring method was used to score the docked poses. DOCK used a combination of van der Waals and electrostatic forces to calculate the energy score for a particular orientation (nonbonded terms of the AMBER force field). The van der Waals potential was approximated using the standard 6−12 Lennard-Jones potential, with 12 as the repulsive exponent and 6 as the attractive exponent. The receptor molecule energy terms were precalculated on a grid to allow for rapid pose scoring, and the sum of these terms were reported as the score. DOCK used up to two scoring methods, the first for initial orientation and minimization and the second for final minimization and ranking of the poses. Energy scoring as described above was used for both scoring methods, not constant scoring.

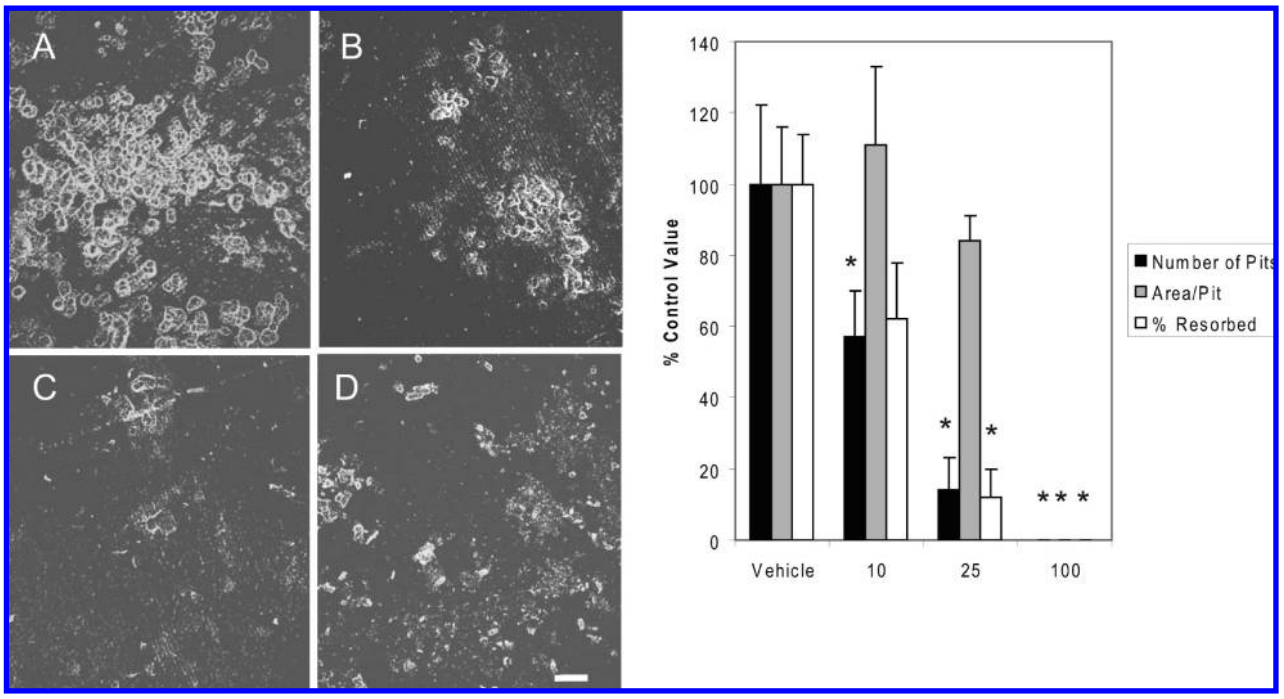

Figure 5. Enoxacin dose dependently reduce bone resorption by mouse marrow cultures. Left panel: scanning electron micrographs of bone slices resorbed by mouse marrow cultures in the presence of vehicle (A), 10 μM enoxacin (B), 25 μM enoxacin (C), 100 μM enoxacin (D). The scale bar = 25 μm. Right panel: tabulation of the percent of the control amount of pit numbers, area per pit, and percent of total area resorbed. The *N* was 4 for each condition.

The bump filter was used to eliminate poses with significant steric overlap prior to the computationally expensive scoring. Orientations rejected during bump filtering were not included in the total count of orientations minimized and scored. If the centers of a ligand atom and probe atom approached closer than 0.75 (75%) of the sum of their van der Waals radii, the position was considered a bump. No more than two bumps were allowed for an initial orientation to be considered valid. These initial bumps were rarely preserved in the final scored poses, as they are energetically unfavorable and such overlaps were resolved during energy minimization.

Actin-Binding Assay. Nineteen molecules were tested for their ability to inhibit interaction between rabbit muscle actin and the *Vma2p*-MBP in a pelleting assay.[14] Briefly *Vma2p*-MBP (1 μM) alone or *Vma2p*-MBP microfilaments (2 μM) were mixed in the presence of 100 μM of each small molecule to be tested or vehicle in an actin polymerizing buffer plus 10 μg/mL phalloidin to maximize filament polymerization. Samples were subjected to ultracentrifugation using a Beckman Airfuge (Beckman Coulter, Fullerton, CA) and pellets and supernatants were collected, subjected to SDS-PAGE, and stained with Comassie Brilliant Blue. Densitometry was performed and the amount (in absorbance units) of *Vma2p*-MBP pelleting in the presence of inhibitor was determined. This was divided by the amount pelleting in the presence of the vehicle, subtracted from 1, and multiplied by 100 to give percent inhibition.

Mouse Marrow Osteoclasts. Mouse marrow osteoclasts were generated as described previously.[29] Swiss-Webster mice (8−20 g) were killed by cervical dislocation, femora and tibia were dissected from adherent tissue, and marrow was removed by cutting both bone ends, inserting a syringe with a 25 gauge needle, and flushing the marrow using αMEM plus 10% fetal bovine serum (αMEM D10). The marrow was washed twice with αMEM D10 and then plated at a density of 1×10^6 cells/cm^2 on tissue culture plates for 5 days in αMEM D10 plus 10^{-8} M 1,25-dihydroxyvitamin D_3 ($1,25D_3$). Cultures were fed on day 3 by replacing half the media per plate and adding fresh $1,25D_3$. After 5 days in culture, osteoclasts appeared. These were detected as giant cells that stained positive for tartrate-resistant acid phosphatase activity (TRAP; a marker for mouse osteoclasts) and overexpressed V-ATPase subunits.[29,30] The University of Florida Institutional Animal Care and Usage Committee approved this protocol.

Actin Rings, Ruffled Membranes, and Resorption Lacunae. To measure actin rings, marrow cells that had been cultured for 5 days with 10^{-8}M $1,25D_3$ on tissue culture plates were scraped and plated onto bone slices in 24-well dishes. Cells were cultured for 5 days in α-MEM D10 plus $1,25D_3$. After incubation, cells were fixed with 2% formaldehyde in PBS for 20 min, permeabilized with 1% Triton X-100 for 10 min, and stained with Texas Red-tagged phalloidin (Sigma) to detect the actin rings.[31] Osteoclasts on bone slices were stained with an anti-E subunit antibody as described previously.[14] The total number of actin rings and ruffled membranes were counted per 1 mm^2 bone slice. Bone resorption was measured by scanning electron microscopy determining the area resorbed by osteoclasts on devitalized mouse cortical bone slices (1 cm^2 × 0.1 mm). Three random 180000 μm^2 photos of each slice were taken at 50×, the images were transferred to Adobe Photoshop, and a grid was superimposed over each picture. Area resorbed was determined by counting the number of grid intersections over pits divided by total grid intersections.

MC3T3-E1 Cell Growth and Mineralization. Mouse MC3T3-E1, subclone 4 preosteoblastic cells were purchased from ATCC (Manassas, VA) and maintained in α-MEM supplemented with 10% fetal bovine serum (FBS; Atlanta Biologicals, Lawrenceville, GA) but which did not include L-ascorbic acid to prevent cell differentiation. The cells were seeded at 1×10^4 cells per cm^2 and maintained at 37 °C in a humidified atmosphere of 95% air and 5% CO_2. All cell cultures were supplemented with 2 mM L-glutamine and penicillin/streptomycin (25 mg/mL). Mineralization was determined by the Von Kossa assay.[32] Briefly, cells were rinsed twice with 1× phosphate buffer saline and fixed in 4% (v/v) paraformaldehyde at room temperature for 10 min.

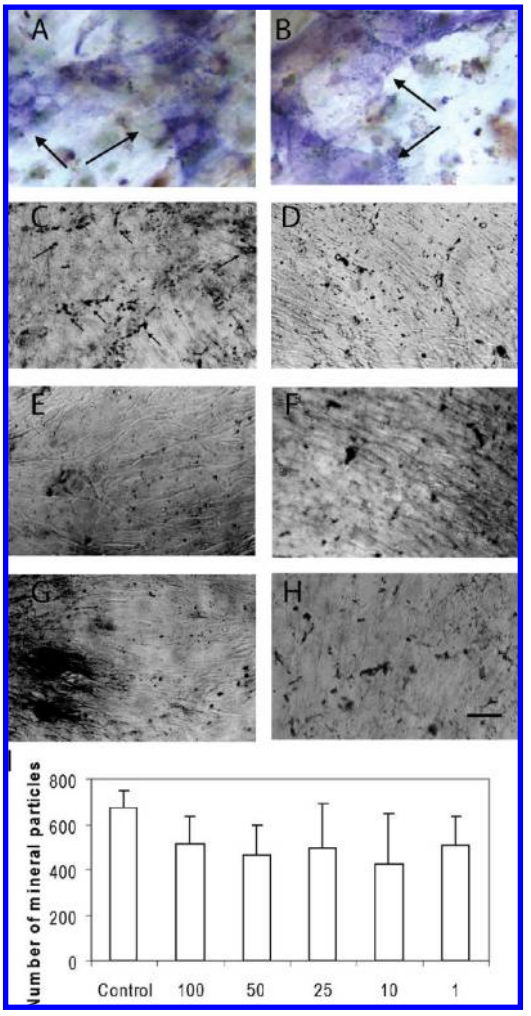

Figure 6. Enoxacin did not block osteoblast formation or mineralization at concentrations where osteoclast numbers were sharply reduced. (A) Typical field from a bone slice with mouse marrow atop a bone slice and cultured in the presence of vehicle fixed and stained after 3 days for alkaline phosphatase activity to detect osteoblasts (blue staining). (B) Typical field from a bone slice in which the cultures were handled identically to A, but in the presence of 10 μM enoxacin. (C−H) Enoxacin had no detected effect on growth and mineralization by MC3T3-E1 subclone 4 osteoblasts at concentrations of 100 μM or less. MC3T3-E1 subclone 4 cells were obtained from ATCC (Manassas, VA) and were inoculated in 24-well plates at a density of 2×10^4 cells/well and were maintained in αMEM D10. To induce mineralization, we treated cultures with with 50 μG/mL ascorbic acid and 10 mM β-glycerophosphate for 15 days. Cells formed monolayers and mineralized in vehicle (C), 100 μM enoxacin (D), 25 μM enoxacin (E), 10 μM enoxacin (F), 5 μM enoxacin (G), and 1 μM enoxacin (H). Mineral deposits were detected as black flecks in all of the images. Some are indicated by small arrows in panel C in order to provide an example. The monolayer of MC3T3 cells appears as striations in the bright field micrographs. The scale bar = 10 μm in A and B and 15 μm in C−H. (I) Quantitation of number of mineral particles per well determined by analysis of Von Kossa stained cells using Image J.

Cells were then rinsed three times in deionized distilled water (ddH_2O), incubated with 5% (w/v) $AgNO_3$ under ultraviolet light (254 nm) for 1 h. Cells were then washed twice with ddH_2O and fixed with 5% sodium thiosulfate for 5 min. Photographs were taken in bright field, transferred to Image J, and mineral flecks were quantititated for three random micrographs per well.

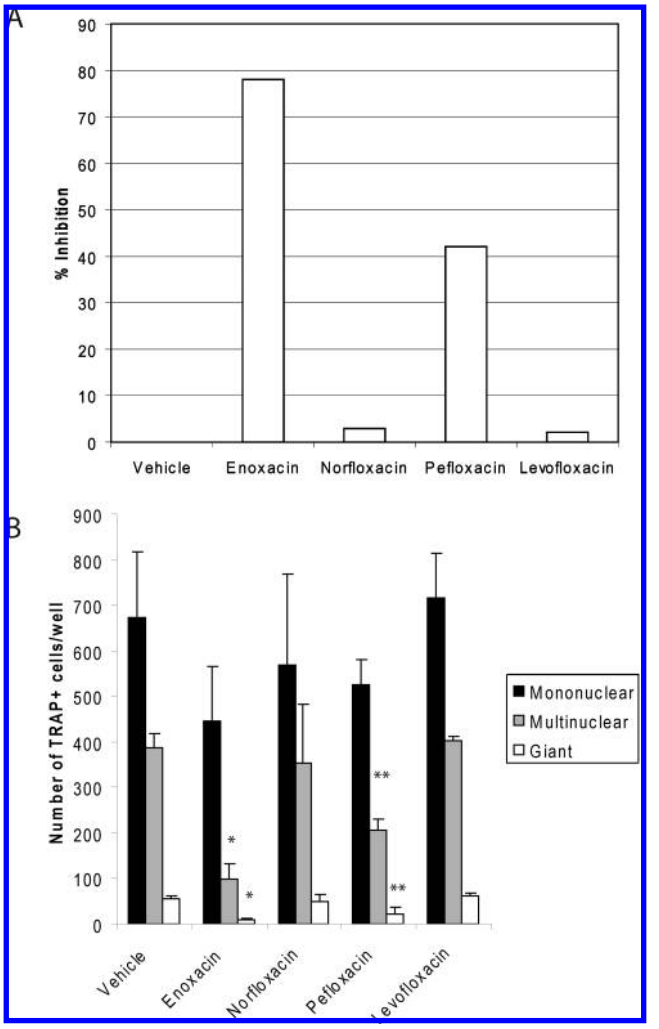

Figure 7. Effects of fluoroquinolones related to enoxacin on interaction between B-subunit and F-actin and on differentiation of mouse marrow osteoclasts. (A) Reduction of B-subunit bound to F-actin in pelleting assay by 100 μM of the various fluoroquinolones. (B) Number of TRAP+ cells per well in the presence of 50 μM of the indicated compound after 6 days in culture. Statistical analysis was performed using Student's t test. Asterisk indicates $P < 0.05$ compared with vehicle control, double asterisk indicates $P < 0.05$ compared with both the vehicle control and with enoxacin.

Acknowledgment. This study was supported by an RGP Opportunity Fund award form the University of Florida.

References

(1) Seeman, E.; Delmas, P. D. Bone quality—the material and structural basis of bone strength and fragility. *N. Engl. J. Med.* **2006**, *354*, 2250–2261.
(2) Mundy, G. R. Osteoporosis and inflammation. *Nutr. Rev.* **2007**, *65*, S147–S151.
(3) Lipton, A.; Jun, S. RANKL inhibition in the treatment of bone metastases. *Curr. Opin. Supportive Palliative Care* **2008**, *2*, 197–203.
(4) Boyce, B. F.; Li, P.; Yao, Z.; Zhang, Q.; Badell, I. R.; Schwarz, E. M.; O'Keefe, R. J.; Xing, L. TNF-alpha and pathologic bone resorption. *Keio J. Med.* **2005**, *54*, 127–131.
(5) Jochum, W.; Passegue, E.; Wagner, E. F. AP-1 in mouse development and tumorigenesis. *Oncogene* **2001**, *20*, 2401–2412.
(6) Novack, D. V.; Teitelbaum, S. L. The osteoclast: friend or foe?. *Annu. Rev. Pathol.* **2008**, *3*, 457–484.
(7) Teitelbaum, S. L. Osteoclasts: culprits in inflammatory osteolysis. *Arthritis Res. Ther.* **2006**, *8*, 201.
(8) Teitelbaum, S. L. Osteoclasts: what do they do and how do they do it? *Am. J. Pathol.* **2007**, *170*, 427–435.

(9) Lee, B. S.; Holliday, L. S.; Krits, I.; Gluck, S. L. Vacuolar H+-ATPase activity and expression in mouse bone marrow cultures. *J. Bone Miner. Res*. **1999**, *14*, 2127–2136.
(10) Blair, H. C.; Teitelbaum, S. L.; Ghiselli, R.; Gluck, S. Osteoclastic bone resorption by a polarized vacuolar proton pump. *Science* **1989**, *245*, 855–857.
(11) Cipriano, D. J.; Wang, Y.; Bond, S.; Hinton, A.; Jefferies, K. C.; Qi, J.; Forgac, M. Structure and regulation of the vacuolar ATPases. *Biochim. Biophys. Acta* **2008**, *1777*, 599–604.
(12) Holliday, L. S.; Lu, M.; Lee, B. S.; Nelson, R. D.; Solivan, S.; Zhang, L.; Gluck, S. L. The amino-terminal domain of the B subunit of vacuolar H+-ATPase contains a filamentous actin binding site. *J. Biol. Chem*. **2000**, *275*, 32331–32337.
(13) Lee, B. S.; Gluck, S. L.; Holliday, L. S. Interaction between vacuolar H(+)-ATPase and microfilaments during osteoclast activation. *J. Biol. Chem*. **1999**, *274*, 29164–29171.
(14) Chen, S. H.; Bubb, M. R.; Yarmola, E. G.; Zuo, J.; Jiang, J.; Lee, B. S.; Lu, M.; Gluck, S. L.; Hurst, I. R.; Holliday, L. S. Vacuolar H+-ATPase binding to microfilaments: regulation in response to phosphatidylinositol 3-kinase activity and detailed characterization of the actin-binding site in subunit B. *J. Biol. Chem*. **2004**, *279*, 7988–7998.
(15) Schluter, K.; Schleicher, M.; Jockusch, B. M. Effects of single amino acid substitutions in the actin-binding site on the biological activity of bovine profilin I. *J. Cell Sci*. **1998**, *111* (22), 3261–3273.
(16) Zuo, J.; Vergara, S.; Kohno, S.; Holliday, L. S. Biochemical and functional characterization of the actin-binding activity of the B subunit of yeast vacuolar H+-ATPase. *J. Exp. Biol*. **2008**, *211*, 1102–1108.
(17) Zuo, J.; Jiang, J.; Chen, S. H.; Vergara, S.; Gong, Y.; Xue, J.; Huang, H.; Kaku, M.; Holliday, L. S. Actin Binding Activity of Subunit B of Vacuolar H(+)-ATPase Is Involved in Its Targeting to Ruffled Membranes of Osteoclasts. *J. Bone Miner. Res*. **2006**, *21*, 714–721.
(18) Schutt, C. E.; Myslik, J. C.; Rozycki, M. D.; Goonesekere, N. C.; Lindberg, U. The structure of crystalline profilin-beta-actin. *Nature* **1993**, *365*, 810–816.
(19) Shan, G.; Li, Y.; Zhang, J.; Li, W.; Szulwach, K. E.; Duan, R.; Faghihi, M. A.; Khalil, A. M.; Lu, L.; Paroo, Z.; Chan, A. W.; Shi, Z.; Liu, Q.; Wahlestedt, C.; He, C.; Jin, P. A small molecule enhances RNA interference and promotes microRNA processing. *Nat. Biotechnol*. **2008**, *26*, 933–940.
(20) Hobert, O. Gene regulation by transcription factors and microRNAs. *Science* **2008**, *319*, 1785–1786.
(21) Zhang, Q.; Zhang, C.; Xi, Z. Enhancement of RNAi by a small molecule antibiotic enoxacin. *Cell Res*. **2008**, *18*, 1077–1079.
(22) Ball, P. Adverse reactions and interactions of fluoroquinolones. *Clin. Invest. Med*. **1989**, *12*, 28–34.
(23) Lomaestro, B. M. Fluoroquinolone-induced renal failure. *Drug Saf*. **2000**, *22*, 479–485.
(24) Rubinstein, E. History of quinolones and their side effects. *Chemotherapy* **2001**, *47* (Suppl. 3), 3–8.
(25) Gluck, S. L.; Lee, B. S.; Wang, S. P.; Underhill, D.; Nemoto, J.; Holliday, L. S. Plasma membrane V-ATPases in proton-transporting cells of the mammalian kidney and osteoclast. *Acta Physiol. Scand. Suppl*. **1998**, *643*, 203–212.
(26) Hiesinger, P. R.; Fayyazuddin, A.; Mehta, S. Q.; Rosenmund, T.; Schulze, K. L.; Zhai, R. G.; Verstreken, P.; Cao, Y.; Zhou, Y.; Kunz, J.; Bellen, H. J. The v-ATPase V-0 subunit a1 is required for a late step in synaptic vesicle exocytosis in *Drosophila*. *Cell* **2005**, *121*, 607–620.
(27) Bordoli, L.; Kiefer, F.; Arnold, K.; Benkert, P.; Battey, J.; Schwede, T. Protein structure homology modeling using SWISS-MODEL workspace. *Nat. Protoc*. **2009**, *4*, 1–13.
(28) Perola, E.; Walters, W. P.; Charifson, P. S. A detailed comparison of current docking and scoring methods on systems of pharmaceutical relevance. *Proteins* **2004**, *56*, 235–249.
(29) Holliday, L. S.; Dean, A. D.; Greenwald, J. E.; Glucks, S. L. C-Type natriuretic peptide increases bone resorption in 1,25-dihydroxyvitamin D3-stimulated mouse bone marrow cultures. *J. Biol. Chem*. **1995**, *270*, 18983–18989.
(30) Holliday, L. S.; Welgus, H. G.; Fliszar, C. J.; Veith, G. M.; Jeffrey, J. J.; Gluck, S. L. Initiation of osteoclast bone resorption by interstitial collagenase. *J. Biol. Chem*. **1997**, *272*, 22053–22058.
(31) Holliday, L. S.; Welgus, H. G.; Hanna, J.; Lee, B. S.; Lu, M.; Jeffrey, J. J.; Gluck, S. L. Interstitial Collagenase Activity Stimulates the Formation of Actin Rings and Ruffled Membranes in Mouse Marrow Osteoclasts. *Calcif. Tissue Int*. **2003**, *72* (3), 206–214.
(32) Jin, D. M.; Chen, L. L.; Yan, J. Effects of IGF-I and BMP-2 combined application on promoting proliferation, differentiation and calcification of MC 3T3-E1 and NIH 3T3 cells. *Zhejiang Da Xue Xue Bao Yi Xue Ban*. **2006**, *35*, 55–63.